



Analysis of Cell Cycle and DNA Compaction Dependent Subnuclear Distribution of Histone Marks

Sunil Kumar Pradhan and M. Cristina Cardoso

Abstract

In eukaryotes, the organization of DNA wrapped around histones regulates DNA-dependent processes. Changes in epigenetic modifications modulate the compaction of DNA into chromatin and, thus, regulate DNA metabolism in time and space. Hence, to catalog the spatiotemporal epigenetic information and its relation to the dynamic nuclear landscape is of paramount importance. Here, we present a method, based on Fiji and the statistical image analysis tool nucim(R), to classify in 3D the nuclear DNA compaction in single interphase cells. We, furthermore, mapped the distribution of (epi)genetic marks and nuclear proteins/processes to the compaction classes along with their dynamics over the cell cycle. These techniques allow to catalog and quantify the dynamic changes in the epigenome in space and time and in single cells.

Key words Cell cycle marker, Confocal microscopy, DAPI, DNA compaction classes, Histone modification, Immunofluorescence, Nuclear marker, Nucleotide labeling

1 Introduction

In eukaryotes, the compacted structure of DNA wrapped around histones is inherently repressive for DNA-dependent processes [1]. However, changes in epigenetic DNA and histone modifications dynamically modulate chromatin compaction [2]. On the one hand, such epigenetic marks need to be maintained over cell division cycles and, on the other hand, such marks need to be reprogrammed during cellular (retro)differentiation. Hence, despite all cells in multicellular organisms having an identical genome, persistent yet plastic epigenetic information regulates when and where cells commit to different lineages with distinct phenotypes [3, 4]. Perturbations in the epigenome can also lead to genome instability, an enabling hallmark of cancer cells [5]. Traditionally, epigenetic information is investigated relative to its role in transcriptional activity. The most studied epigenetic mark with a clear

relationship to gene transcription is the acetylation of histones by histone acetyltransferases (HAT) and the removal of this modification by deacetylase (HDAC) enzymes. A high level of acetylation correlates with transcriptional activity and a low acetylation level with gene repression [6]. On the other hand, the dynamics and influence of epigenetic changes on cell cycle progression and metabolic processes such as DNA replication and repair remain unclear. Hence, the need to catalog epigenetic information in space and time and its relation to the dynamic nuclear landscape has become a new and rapidly progressing field of research [7].

Developments in single-cell chromatin accessibility and next-generation sequencing paved the way to independently map the chromatin state of individual cells [8]. However, these methods are lacking in spatial information and suffer from a loss of information, especially for the chromatin state of repetitive DNA elements. The latter constitute the largest chunk of heterochromatin across species and play a crucial role in genome stability [9]. Microscopic techniques are the most suited to map the spatiotemporal chromatin state in a 3D preserved cell. Advances in conventional and super-resolution microscopy are proving to be reliable tools to study chromatin structure and epigenetic information in 3D preserved cells and live cells, hence dissecting the tight-knit dynamics of different factors [10]. In past years, different microscopy tools have been used to dissect chromosome territories (CT) and the basic unit of CT; the chromatin domains (CD) [11, 12]. Based on these, the functional nuclear organization is composed of two spatially co-aligned active and inactive nuclear compartments (ANC-INC). The INC is composed of compacted parts of chromatin domain clusters (CDCs) which are transcriptionally incompetent and enriched in repressive histone marks. The ANC includes the interchromatin compartment (IC) which is largely devoid of chromatin and decondensed, transcriptionally competent periphery of chromatin domain clusters or perichromatin region (PR). A combined approach of detecting and quantifying epigenetic information and the functional genome organization over the cell cycle in a 3D preserved cell would be powerful enough to uncover the interaction of multiple factors simultaneously and shed light on their dynamics across time.

For a long time, the DNA marker DAPI has been extensively used for cell cycle profiling and distinguishing subnuclear structures like heterochromatin clusters (i.e., chromocenters) [13]. Albeit exhibiting a bias towards AT-rich DNA sequences, DAPI intensity works as a proxy for the condensation level of chromatin. Recently, the DNA in the whole cell nucleus was classified into different compaction classes based on the DAPI intensity [14, 15]. Harnessing the power of advanced microscopy and statistical image analysis, different DNA compaction classes were defined, reflecting the 3D subnuclear compartmentalization

landscape in single cells. Nucleome imaging toolbox (Nucim) is a statistical tool for (semi)-automated 3D quantitative image analysis of the spatial organization of DNA in the nucleus developed on the open statistical analysis tool R [15, 16]. This tool enables quantifying the super-resolved chromatin compaction classes in individual nuclei. Instead of the commonly used intensity threshold-based algorithms, the tool assigns each voxel into a certain class based on the probability of this voxel belonging to the same class computed from a stochastic model called the hidden Markov random field (HMRF) model, eventually classifying the nucleus into a pre-defined number of segmented classes. This feature compensates for the cell-to-cell DAPI intensity variation that can arise from various factors including human error. In addition, the tool also allows mapping and quantifying the relative fraction of total voxels from DNA sequences (based on fluorescence in situ hybridization), (in)-active nuclear marks (e.g., methylated or acetylated histones), epigenetic modifications, chromatin architectural proteins (CTCF, SAF-A) and nucleotide analogs (EdU) incorporated into DNA during replication within individual DNA compaction classes.

In this chapter, we present the use of the statistical tool “nucim” to classify the nuclear DNA compaction based on DAPI images acquired from the more commonly used confocal microscopy systems. We also mapped the corresponding enrichment of histone marks and their S-phase-specific replication timing. For precise quantification of the classes, the nucleus was separately segmented and a DAPI mask was created in the open image analysis tool Fiji [17]. Afterward, the DAPI mask was imported into R along with the original image to classify the nucleus into seven different compaction classes (Fig. 1). The classification profiles are comparable to the previously analyzed profiles from super-resolved DAPI images [14]. Compaction class one represents the interchromatin compartment (IC) and the nucleolus, which are largely devoid of chromatin. Compaction classes two to seven represent the chromatin with increasing DAPI intensity, which acts as a proxy for increasing levels of chromatin condensation. Classes two, three, and four represent the decondensed chromatin which is transcriptionally competent and enriched in active chromatin marks (e.g., acetylated histones), hence acting as a proxy for the active nuclear compartment (ANC). The last three compaction classes represent the condensed, transcriptionally repressed inactive nuclear compartment (INC). With an automated threshold/intensity-based approach, colors from green or red channels were segmented and the voxels were mapped to different compaction classes. The threshold-based approach is useful for quantifying the relative fraction of signal voxels from pre-segmented images (segmented foci or signals in Fiji or Volocity) in individual compaction classes. The intensity-based approach (recommended) is a combination of two approaches, where, first, a semiautomatic (or manual) threshold is

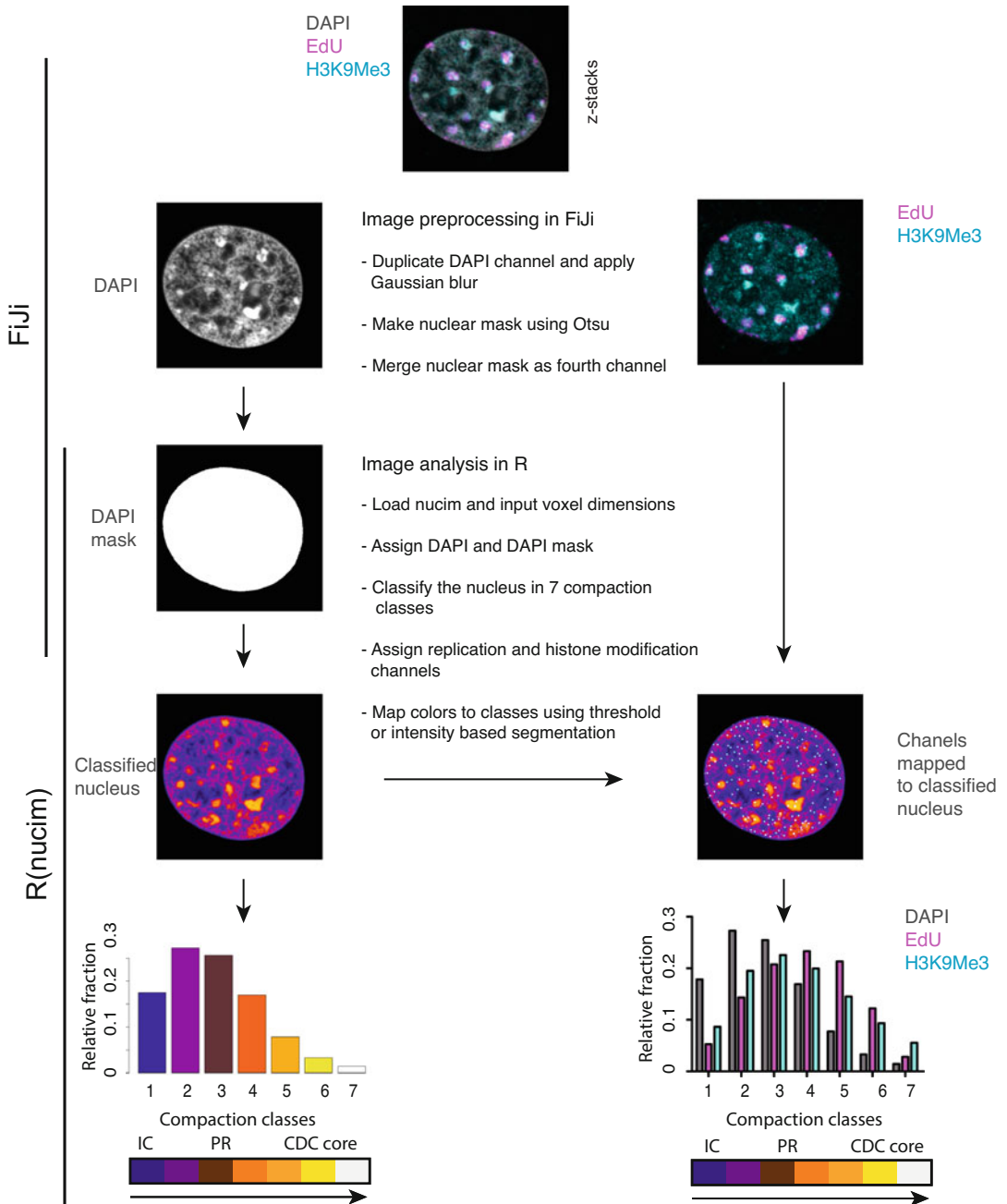


Fig. 1 Preprocessing and quantitative analysis pipeline for mapping chromatin marks to compaction classes: In Fiji, using the Gaussian blur followed by auto-threshold (otsu), the nucleus was segmented, binarized, and holes were filled. All channels were converted to grey using LUT. In R, the TIFF file was imported after loading libraries, voxel size was defined, and the nucleus was classified into seven chromatin compaction classes representing (in)active nuclear compartments. Class one represents the DNA-free interchromatin compartment (IC) and nucleolus. Classes two, three, and four represent the transcriptionally competent perichromatin region (PR). The last three classes represent the inactive nuclear compartment (CDC core). Using a threshold/intensity-based segmentation signal from EdU (replication)/H3K9me3 (histone modification), channels were mapped to compaction classes

applied to identify the colors (DNA, RNA, or protein). This is followed by an intensity-weighted calculation of the relative fraction, leading to more intense signals having a larger impact and low-intensity signals having less impact. Distinct euchromatin and heterochromatin marks can be mapped to different compaction classes. A cell cycle marker or replication progression marker (nucleotide analogs like EdU or replisome machinery components like PCNA) gives the spatiotemporal distribution of these marks as these define the progression of the cell cycle. With advances in 3D live-cell microscopy, the development of live-cell specific fluorescent DNA dyes (SiR Hoechst, DRAQ5) [18], and incorporation of fluorescently-tagged proteins (epigenetic readers and writers, DNA replication, and transcription machinery), nucim enables to catalog the dynamic 3D spatial distribution of multiple factors with respect to the dynamic chromatin. Here, we show the application of this method to the quantification of euchromatin/heterochromatin marks throughout the cell cycle. We classified mouse myoblast nuclei into seven compaction classes and mapped histone marks into compaction classes during the progression of DNA replication (Fig. 2a). Relative fractions of H4K8ac mapped in the early S-phase were higher in classes two, three, and four, marking open chromatin. In the mid S-phase (marked by replicating inactive X chromosome), facultative heterochromatin mark H3K27me3 was enriched in classes three, four, and five. Interestingly, the relative fractions of EdU were comparatively higher in classes four and five. The constitutive heterochromatin mark H3K9me3 mapped to compaction classes in late S-phase cells (marked by replicating chromocenters) was higher in the last three compaction classes, which represent the inactive nuclear compartments (Fig. 2b).

All in all, this analysis strategy enables quantitative 3d compaction classification of the interphase nucleus, distribution of (epi)genetic marks, and nuclear proteins/processes in the compaction classes along with their dynamics over the cell cycle from images taken from both fixed cell and live-cell confocal microscopy. This method, thus, allows to catalog and quantify the dynamic changes in the epigenome with respect to the cell cycle stages.

2 Materials

Prepare all solutions at room temperature unless otherwise noted. All solutions and materials that come into contact with live cells must be sterile and have to be handled inside a tissue culture biosafety cabinet. Disposal of reagents, solutions, and cell material should be carried out following the specific regulations in effect.

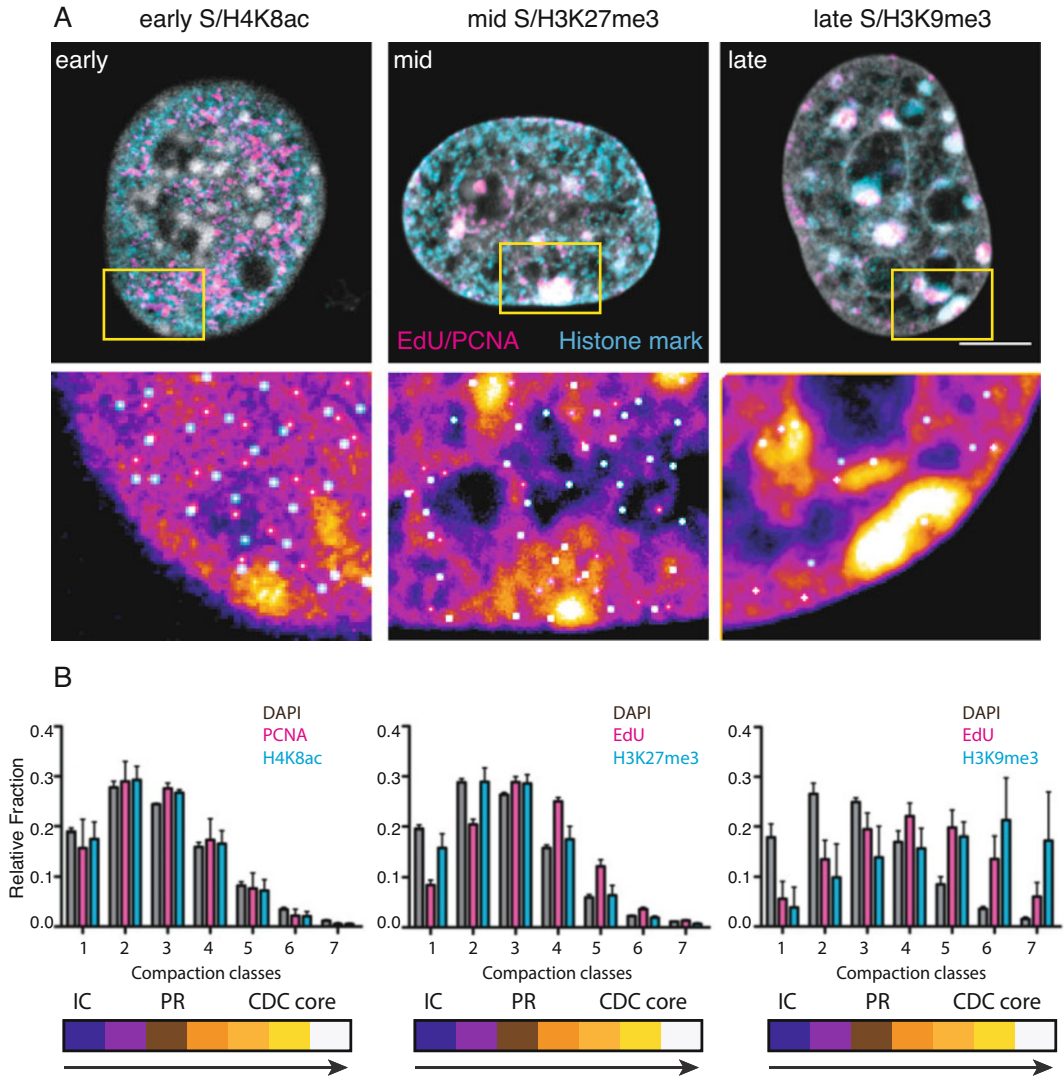


Fig. 2 Using Fiji and R (nucim), the nucleus was classified into seven different chromatin compaction classes. Euchromatin (H4K8ac), facultative heterochromatin (H3K27me3), and constitutive heterochromatin (H3K9me3) marks were mapped to compaction classes (see also Fig. 1). **(a)** mouse myoblast cells in early, mid (marked by replicating Xi, within the box), and late S-phase (marked by replicating constitutive heterochromatin termed chromocenters) stained with H4K8ac, H3K27me3, and H3K9me3, respectively. Representative segmented replication foci (RFi, magenta) and histone modification (cyan) corresponding to different compaction classes. **(b)** RFi and histone modifications mapped to different chromatin compaction classes. The relative fraction of H4K8ac is higher in the first four classes and correlated to the RFi relative fraction. H3K27me3 is higher in classes two, three, and four, but RFi was higher in classes three, four, and five. H3K9me3 and RFi relative fractions are higher in the last four chromatin compaction classes

2.1 Cell Culture

1. Cells of interest (in our example, C2C12 female mouse myoblast cells) [19]
2. Standard cell culture media and supplements. For C2C12: Dulbecco's Modified Eagle Medium (high glucose, DMEM, Sigma-Aldrich, St Louis, MO, USA) supplemented with 20% fetal bovine serum, $1 \times$ glutamine (cat# G7513, Sigma-Aldrich, St Louis, MO, USA), and $1 \mu\text{M}$ gentamicin (cat# G1397, Sigma-Aldrich, St Louis, MO, USA).
3. Borosilicate glass coverslips, round or square.
4. UV crosslinker to disinfect the coverslips.

2.2 RFI Labeling and Detection

1. Cell permeable nucleoside EdU (5-ethynyl-2'-deoxyuridine) stock solution 10 mM in DMSO. EdU-Click IT detection kit (Carl Roth, catalog # 7773.1) (*see Note 1*).
2. For detection of replisome protein: mouse monoclonal anti-PCNA antibody (Santa Cruz, catalog # sc-056).

2.3 Immunofluorescence

1. $1 \times$ PBS: 8 g NaCl, 0.2 g KCl₂, 17 g Na₂HPO₄ \times 7H₂O, 0.2 g KH₂PO₄ per liter of ddH₂O, pH \sim 6.8, prepare from autoclaved $10 \times$ stock solution.
2. Permeabilization buffer: 0.5% TritonX-100 solution in $1 \times$ PBS buffer.
3. 37.5% formaldehyde in ddH₂O (Sigma).
4. Wash buffer PBST: $1 \times$ PBS, 0.01% Tween.
5. Blocking buffer: 0.5% fish skin gelatin/4% BSA in $1 \times$ PBS.
6. Primary antibodies: anti-histone H3 K9 trimethyl (mouse monoclonal, Active Motif, catalog# 39285), anti-histone H3 K27 trimethyl (rabbit polyclonal, Upstate, catalog# 07-449), anti-histone H4 K8 acetyl (rabbit polyclonal, Upstate, catalog# 06-760).
7. Secondary antibodies: a diverse array of secondary antibodies can be used. Here we used anti-mouse IgG Alexa Fluor 488 (goat polyclonal, Invitrogen, catalog#A11029), anti-rabbit IgG Alexa Fluor 488 (donkey polyclonal, Invitrogen, catalog#A11034) (*see Note 2*).
8. DAPI or 4',6-diamidino-2-phenylindole dihydrochloride (350/461 nm excitation/emission maxima, respectively): final concentration of $1 \mu\text{g}/\text{mL}$ in ddH₂O (Sigma, catalog# D8417-5MG).
9. Microscope slides (Thermo scientific, catalog # ABAA000080).
10. Vectashield antifade mounting media (Vector Labs, catalog # VEC-H-1000) (*see Note 3*).

11. Transparent nail polish from drugstore.
12. Humidified staining chamber (*see* **Note 4**).

2.4 Microscopy and Image Analysis

1. Any point scanning or spinning disk confocal microscope with a high magnification objective (e.g., 60× or 100×) is recommended. In our case, we use a Leica SP5 II confocal microscope equipped with an HCX PL APO 100×/1.44 oil objective.
2. Multispectral fluorescent beads (PS-Speck microscope point source kit Invitrogen, P7220).
3. Image acquisition software. In our case, we use LAS AF (Leica microsystems).
4. FiJi for image preprocessing (<https://fiji.sc/>).
5. R for image analysis and statistics (<https://www.r-project.org/>).
6. Nucim for image analysis (<https://bioimaginggroup.github.io/nucim/>).
7. Prism (optional) for statistical analysis (<https://www.graphpad.com/scientificsoftware/prism/>).

3 Methods

3.1 Cell Culture

The protocol uses adherent cells. For cells in suspension, a separate protocol involving a cytopsin step can be used. It is crucial not to allow the culture to become too confluent. All solutions used in cell culture should be warmed to 37 °C prior to use. Cells are incubated at 37 °C in a humidified atmosphere with 5% CO₂ in the appropriate culture media.

1. Sterilize the coverslips inside the UV crosslinker for 30 min.
2. Seed the cells at 50–70% confluency onto UV-sterilized coverslips and let them adhere overnight in the respective media (*see* **Note 5**).
3. Add nucleoside analog EdU to the media at a final concentration of 10 μM for about 10–15 min (*see* **Note 6**).
4. Meanwhile, prepare the fixative solution by diluting the 37.5% formaldehyde to 3.75% in 1× PBS.
5. Remove media and wash the cells with 1× PBS.
6. Remove PBS and fix the cells with the fixative solution for 10 min (*see* **Note 7**).

3.2 Immunostaining

For immunostaining, all incubations are done at room temperature and in the dark unless otherwise noted.

1. After fixation, wash the cells with 1× PBS thrice for 5 min each time.

2. Permeabilize the cells with the permeabilization buffer for 15 minutes.
3. Wash the cells with $1 \times$ PBS thrice for 5 min each time.
4. At this point, you can take individual coverslips from the culture dishes into a humid staining chamber (*see Note 4*).
5. Incubate the cells with a blocking buffer for 30 min.
6. Stain with the primary antibody diluted in blocking buffer for 1 h.
7. Wash with PBST thrice for 10 min each time.
8. Stain with the secondary antibodies diluted in blocking buffer for 1 h.
9. Wash with PBST thrice for 10 min each time, add EdU-Click IT detection solution for 30 min and wash again with PBST.
10. Incubate with 20–50 μ L (depending on coverslip size) of the DAPI solution for 10 min.
11. Meanwhile take out a glass slide and put a drop of Vectashield mounting medium on top (*see Note 3*).
12. Briefly wash with ddH₂O, dry excess water on a paper tissue, and place on top of the mounting medium with the cells' side facing down (*see Note 8*).
13. Seal the coverslip to the slide with transparent nail polish (*see Note 9*).

3.3 Image Acquisition

The microscope to be used should be aligned for Köhler illumination. One should also calibrate the alignment between channels using multi-spectral fluorescent beads (*see Note 10*).

The objectives should be cleaned with ethanol using lint-free wipes before and after use.

1. Set up the image acquisition settings for each channel and use the same setting for all the acquisitions as follows:
 - It is crucial to avoid oversaturation of the images and bleed-through signals from other fluorophores (*see Note 11*).
 - Acquire images in sequential order from higher wavelength to lower wavelength, e.g., starting with red, green, and acquiring blue at the end (*see Note 12*).
 - The images should be of the same size, e.g., if you are using zoom factor 5 in a point scanner system, you should keep it for all the images (*see Note 13*).
 - Keep the Z slice distance constant, and it should be according to the Nyquist limit (*see Note 14*).
2. Acquire the images in such a way that there should be one cell in each image, and it should be at the center. The Z stacks should cover the whole cell.

3. Save the images in the prescribed formats (e.g., TIFF, LIF) and avoid any form of compression or manipulation of the intensity levels.

3.4 Image Preprocessing in Fiji

Image preprocessing can be done using Fiji. First, all raw formats (.LIF, .nd2) should be converted to .tiff and saved for processing (Fig. 1). The goal is to delete unnecessary slices above and below the nucleus, followed by creating a nuclear mask to be later used for classification.

1. Open the images in Fiji using “Drag and Drop” or using “Bio format importer.”
2. Slice out the unnecessary slices and crop images if necessary.
3. Split the channels: Image>Color>Split Channels.
4. Duplicate the DAPI channel: Image>Duplicate.
5. Process the image with a filter algorithm (mean/Gaussian blur): Process>Filter>Gaussian blur (Sigma: 2, process all images: yes).
6. Apply threshold to segment the nucleus: Image>Adjust>Auto Threshold (Method: Otsu, White objects on black background, Stack, Use stack histogram).
7. Convert to mask: Process>Binary>Convert to mask.
8. The above step should give a binary image. To fill holes in the mask: Process>Binary>Fill holes (process all images: yes).
9. Merge the three channels with the DAPI mask as a fourth channel: Image>Color>Merge channels (create composite).
10. Convert the color of all channels to grey using LUT (*see Note 15*).
11. Save the image as TIFF.

3.5 Image Analysis in R (Workflow for a Single Cell)

It’s recommended to use Rstudio for a better user interface. The object is to define the voxel size of the images, classify the nucleus using the nuclear mask, followed by mapping the colors to individual classes.

1. Open R (version 4.1.0) or Rstudio.
2. Install “nucim” as follows:

```
setRepositories(ind=c(1,2))
install.packages("nucim")
or
```

One can install as follows in Rstudio:

```
Packages > Install > nucim (check "Install dependencies") >
Install
```

3. Load the libraries:

```
library(bioimager)
library(nucim)
```

4. Import the image to R:

```
img = readTIF(file.choose())
```

Here, you have to choose the particular image by going into the folder. One can also directly assign the path.

5. Add the dimensions of the voxels in microns (*see Note 16*):

```
x = y = 0.0433
```

```
z = 0.2937
```

6. Define DAPI/blue channel and the nuclear mask:

```
blue= img[,3,]
```

```
mask= img[,4,]
```

7. Classify the nucleus into seven compaction classes using the classify function and DAPI mask. Here, one can also change the number of classes to 5 or 9 instead of 7 (*see Note 17*):

```
classes = classify (blue, mask, 7, beta = 0.1, z=x/z)
```

8. From the resulting object, where each voxel inside the mask is assigned to a class, count the percentage of voxels in each class and plot it:

```
tab<-table.n(classes, 7, percentage=TRUE)
```

```
barplot(tab, ylab="percentage", xlab="chromatin compaction level", col=heatmap.color(7))
```

9. To map the colors into classes, define the colors and choose the threshold or intensity approach to plot the percentage.

```
red = img[,1,]
```

```
green = img[,2,]
```

```
cc1<-colors.in.classes(classes, red, green, mask, 7, type="-  
thresh", plot=TRUE,  
col1="red", col2="green", thresh1=0.15, thresh2=0.15,
```

```
test="Wilcoxon",ylim=c(0,.5),
xlab="chromatin compaction levels",ylab="percentage")
```

OR

```
cc1<-colors.in.classes(classes,red,green,mask,7,type="inten-
sity",plot=TRUE,
coll="red",col2="green",thresh1=0.15,thresh2=0.15,
test="Wilcoxon",ylim=c(0,.5),
xlab="chromatin compaction levels",ylab="percentage")
```

3.6 Image Analysis in R (Workflow on a Batch of Cells)

1. For batch analysis of a set of cells present in a folder, use the same method as above but looped. This will automatically classify the individual nuclei, map the colors into classes, and generate the respective .csv files for each color (e.g., DAPI, EdU, histone) in the working directory chosen. For individual nuclei, there should be seven (depending on the number of classes one chooses to classify into) probability values where the first is for class one and the last for class seven.

```
files = list.files(path="path to the folder ", pattern="*.
tif", full.names=TRUE, recursive=FALSE)

for (f in files){
  print(substring(f, first = 50))
  img= readTIF(f)
  x = y = 0.0433
  z = 0.2937
  blue = img[,3,]
  mask = img[,4,]
  classes = classify(blue, mask, 7, beta=0.1, z=x/z)
  tab<-table.n(classes, 7, percentage=TRUE)
  par(pty="s")
  red = img[,1,]
  green = img[,2,]
  cc1<-colors.in.classes(classes,red,green,mask,7,type="inten-
sity",plot=TRUE,
coll="red",col2="green",thresh1=0.15,thresh2=0.15,
test="Wilcoxon",ylim=c(0,.5),
xlab="chromatin compaction levels",ylab="percentage")
  write.table(t(cc1$dapi), file = 'DAPI.csv', sep = ',', append
= TRUE, col.names = FALSE)
  write.table(t(cc1$coll), file = 'EdU.csv', sep = ',', append =
TRUE, col.names = FALSE)
  write.table(t(cc1$col2), file = 'Histone.csv', sep = ',',
append = TRUE, col.names = FALSE)

  print('-----')
}
```

2. Go to the chosen directory to import the values to R or Prism to plot for the whole folder. You will find seven different values belonging to seven different classes, respectively.

4 Notes

1. EdU is recommended instead of BrdU, as denaturation of DNA is required for BrdU detection. This can affect the nuclear DNA distribution.
2. Depending on the primary antibody, one can choose fluorescently conjugated secondary antibodies with no spectral overlap between themselves for multiple antibody stainings and with no spectral overlap with the EdU detection reagent and with DAPI. The choice depends also on the illumination and detection possible in the microscopy systems available.
3. Vectashield is light-sensitive. Put it on the slide a few moments before mounting. Other mounting media like mowiol can be used but may flatten the sample.
4. Avoid long exposure of fluorochrome-conjugated reagents to light and drying out of the samples. All immunofluorescence steps should be done in a humidified dark chamber [20].
5. Cells should be seeded in a way that they are not too confluent to avoid contact inhibition and cell cycle stop. For embryonic stem cells, which grow in colonies, one can seed for 8–12 h on gelatin-coated coverslips before fixing.
6. In mammalian cells, 10–15 min of nucleotide incorporation marks individual replication foci (RFis) and gives a distinct spatial pattern that marks early, mid, or late S-phase. Instead of EdU, one can also immunostain for the replisome component PCNA (the DNA polymerase processivity clamp), which gives similar results. For detecting replication-associated PCNA, one can fix the samples with 3.75% formaldehyde followed by treating the cells with 100% ice-cold methanol for 10 min.
7. The fixative solution should be freshly prepared. Alcohol-based fixatives like methanol or ethanol are not as suited as they usually flatten the nuclei.
8. Let the Vectashield spread throughout the coverslips for a few minutes so that there are no bubbles inside before drying them out. Flip upside down and press gently on the tissue paper to get rid of any bubbles.
9. This step is not required if the mounting media chosen can harden and create a permanent seal.
10. There must be no misalignment between channels as the method maps spots to different DAPI classes. If there is a

shift and the pixel shift is calibrated, the realignment can be done in Fiji by Image> Transform> Translate (bicubic interpolation). Realignment through Z is also possible in Fiji by shifting slices through the Z-axis.

11. As the DAPI signal will be divided into seven classes, oversaturating the image would result in assigning a maximum percentage of voxels into the higher compaction classes, and information would be lost.
12. In the classic confocal microscopes, one can avoid bleed-through fluorescence emission by sequentially taking the images, controlling the laser power, and adjusting the bandwidth. For the spinning disc system, one can reduce the exposure time.
13. To analyze all the cells in a folder, one has to keep the voxel size the same. Changing the zoom factor or changing the size of the Z-slice would affect the analysis. Cropping the already acquired images does not affect this.
14. Based on the microscopic parameters (such as numerical aperture, excitation/emission wavelengths, refractive index, etc.), one can determine the voxel size to acquire according to the Nyquist criterion, hence avoiding oversampling or undersampling.
15. In R, to recognize the mask as a fourth channel, all individual channels should be manually converted to gray using the LUT editor.
16. The information about voxel sizes can be found in Fiji as follows: Image> Show info.
17. Before batch analysis, one can test one sample for classification and mapping the channels to classes. Here, one can look at which method (threshold/intensity) is most suited for the analysis.

Acknowledgments

We thank Haris Kujundzic for the initial testing of the method, Corella S. Casas-Delucchi for image data, Alexander Rapp, Cathia Rausch, and Maria Arroyo for many useful comments and all present and past members of the laboratory for their contributions over the years. The laboratory of M. Cristina Cardoso is supported by grants from the German Research Foundation (DFG Project-ID 393547839 – SFB 1361, CA 198/9-2, and CA 198/12-1), the Federal Ministry of Education and Research (BMBF), and the Hessian Ministry of Higher Education, Research, Science, and the Arts (HMWK).

References

- Kornberg RD (1974) Chromatin structure: a repeating unit of histones and DNA. *Science* 184:868–871. <https://doi.org/10.1126/science.184.4139.868>
- Allshire RC, Madhani HD (2018) Ten principles of heterochromatin formation and function. *Nat Rev Mol Cell Biol* 19:229–244. <https://doi.org/10.1038/nrm.2017.119>
- Mikkelsen TS, Ku M, Jaffe DB et al (2007) Genome-wide maps of chromatin state in pluripotent and lineage-committed cells. *Nature* 448:553–560. <https://doi.org/10.1038/nature06008>
- Heintzman ND, Hon GC, Hawkins RD et al (2009) Histone modifications at human enhancers reflect global cell-type-specific gene expression. *Nature* 459:108–112. <https://doi.org/10.1038/nature07829>
- Hanahan D, Weinberg RA (2011) Hallmarks of cancer: the next generation. *Cell* 144:646–674. <https://doi.org/10.1016/j.cell.2011.02.013>
- Kuo MH, Allis CD (1998) Roles of histone acetyltransferases and deacetylases in gene regulation. *BioEssays* 20:615–626. [https://doi.org/10.1002/\(SICI\)1521-1878\(199808\)20:8<615::AID-BIES4>3.0.CO;2-H](https://doi.org/10.1002/(SICI)1521-1878(199808)20:8<615::AID-BIES4>3.0.CO;2-H)
- Tashiro S, Lanctôt C (2015) The international nucleome consortium. *Nucleus* 6:89–92. <https://doi.org/10.1080/19491034.2015.1022703>
- Buenrostro JD, Wu B, Litzenburger UM et al (2015) Single-cell chromatin accessibility reveals principles of regulatory variation. *Nature* 523:486–490. <https://doi.org/10.1038/nature14590>
- Jagannathan M, Cummings R, Yamashita YM (2018) A conserved function for pericentromeric satellite DNA. *eLife* 7:e34122. <https://doi.org/10.7554/eLife.34122>
- Schermelleh L, Heintzmann R, Leonhardt H (2010) A guide to super-resolution fluorescence microscopy. *J Cell Biol* 190:165–175. <https://doi.org/10.1083/jcb.201002018>
- Cremer T, Cremer C (2001) Chromosome territories, nuclear architecture and gene regulation in mammalian cells. *Nat Rev Genet* 2:292–301. <https://doi.org/10.1038/35066075>
- Cremer T, Cremer M, Hübner B et al (2015) The 4D nucleome: evidence for a dynamic nuclear landscape based on co-aligned active and inactive nuclear compartments. *FEBS Lett* 589:2931–2943. <https://doi.org/10.1016/j.febslet.2015.05.037>
- Kapuscinski J (1995) DAPI: a DNA-specific fluorescent probe. *Biotech Histochem* 70:220–233. <https://doi.org/10.3109/10520299509108199>
- Smeets D, Markaki Y, Schmid VJ et al (2014) Three-dimensional super-resolution microscopy of the inactive X chromosome territory reveals a collapse of its active nuclear compartment harboring distinct Xist RNA foci. *Epigenetics Chromatin* 7:8. <https://doi.org/10.1186/1756-8935-7-8>
- Schmid VJ, Cremer M, Cremer T (2017) Quantitative analyses of the 3D nuclear landscape recorded with super-resolved fluorescence microscopy. *Methods* 123:33–46. <https://doi.org/10.1016/j.ymeth.2017.03.013>
- R Core Team (2013) R: A language and environment for statistical computing. R Foundation for Statistical Computing, Vienna
- Schindelin J, Arganda-Carreras I, Frise E et al (2012) Fiji: an open-source platform for biological-image analysis. *Nat Methods* 9:676–682. <https://doi.org/10.1038/nmeth.2019>
- Martin RM, Leonhardt H, Cardoso MC (2005) DNA labeling in living cells. *Cytometry A* 67:45–52. <https://doi.org/10.1002/cyto.a.20172>
- Yaffe D, Saxel O (1977) Serial passaging and differentiation of myogenic cells isolated from dystrophic mouse muscle. *Nature* 270:725–727. <https://doi.org/10.1038/270725a0>
- Cardoso MC, Leonhardt H (1996) Immunofluorescence techniques in cell cycle studies. In: Pagano M (ed) *Cell cycle—materials and methods*. Springer, Berlin Heidelberg, pp 15–28